ELSEVIER

Journal of Chromatography A, 813 (1998) 1–9

JOURNAL OF CHROMATOGRAPHY A

Detailed study of the mass transfer kinetics of Tröger's base on cellulose triacetate

Preshious Rearden[a,b], Peter Sajonz[a,b], Georges Guiochon[a,b,*]

[a]*Department of Chemistry, University of Tennessee, Knoxville, TN 37996-1600, USA*

[b]*Chemical and Analytical Science Division, Oak Ridge National Laboratory, Oak Ridge, TN 37831-6120, USA*

Received 3 December 1997; received in revised form 20 March 1998; accepted 30 March 1998

Abstract

The adsorption isotherm of *S*-Tröger's base on microcrystalline cellulose triacetate was measured by frontal analysis at several flow-rates between 0.2 and 1.2 ml/min. Two chromatographic models were used in order to study the kinetics of mass transfer between the two phases and to derive plate height values, the equilibrium–dispersive model and the transport model of chromatography. The dependence of the plate height on the flow velocity and on the solute concentration was studied. A modified Van Deemter equation was used to separate the contributions due to slow mass transfer and to axial dispersion.

Keywords: Mass transfer; Kinetic studies; Adsorption isotherms; Axial dispersion; Stationary phases, LC; Cellulose triacetate stationary phase; Tröger's base

1. Introduction

Microcrystalline cellulose triacetate (CTA) has been widely used for several years in liquid chromatography as a stationary phase for enantiomeric separations [1–5]. Its popularity is due to the combination of its high enantioselectivity for many groups of compounds, its high loadability, its good mechanical stability, and its relatively low cost compared to more conventional chiral phases [4]. Despite these important advantages, this stationary phase is more often used for preparative than for analytical applications because an unusually low column efficiency is often reported. This poor efficiency drastically limits column performance. No convincing explanation is yet found in the literature to explain the origin of the important peak broadening observed when using CTA.

The separation of the *R*- and *S*-enantiomers of Tröger's base (TB) on CTA has been studied previously [6,7]. This system was shown to exhibit an unusual separation behavior under nonlinear conditions. The separation between the bands of the two enantiomers increased with increasing sample size until a certain size was reached, beyond which normal behavior was resumed and the resolution between the two bands decreased with increasing sample size. This unusual behavior is due to the fact that, under the experimental conditions of that investigation (25°C), the isotherms of the two enantiomers belong to different types. The adsorption isotherm of the (−)- or *S*-enantiomer was well

*Corresponding author. Address for correspondence: Department of Chemistry, University of Tennessee, Knoxville, TN 37996-1600, USA.

0021-9673/98/$19.00
PII: S0021-9673(98)00253-2

described by the Langmuir equation while that of the (+)- or *R*-enantiomer was accounted for by a quadratic equation leading to an *S*-shaped isotherm [6,7]. The mass transfer kinetics in this system was also reported to be strongly concentration dependent [8], an observation which has been repeated for other systems [9].

In this paper we investigate the mass transfer kinetics of the *S*-enantiomer of Tröger's base in the system ethanol–CTA. We compare two different ways to determine the isotherm data for this enantiomer, study the dependence of the isotherm data on the flow-rate, compare the performance of two conventional models of nonlinear chromatography (the equilibrium–dispersive and the transport models) in accounting for the band profiles, and discuss the influence of the solute concentration on the rate coefficient of mass transfer and on the column height equivalent to a theoretical place (HETP).

2. Theory

2.1. The equilibrium–dispersive and the transport models of chromatography

We used these two different models to account for the experimental results. Each model is characterized by one parameter, the apparent dispersion factor and the apparent mass transfer coefficient, respectively. For each experiment, the best value of the parameter of each model is derived by identification of the experimental breakthrough curves obtained in frontal analysis to a numerical solution of the model. Each model provides for the derivation of the column HETP under linear conditions. This concept can be extended to the nonlinear case with some care [7]. We expect the values of the HETP obtained with both models to be closed. However, this comparison, which presents much interest from a theoretical viewpoint, has never been done yet. There has even been some suspicion that the unexpected concentration dependence of the rate coefficient of mass transfer kinetics previously reported [8,9,13] is due to a model error. A comparison between the two sets of results obtained in this process could contribute to clarify this issue.

2.1.1. Mass balance equation

The mass balance equation of both models is written as

$$\frac{\partial C}{\partial t} + F\,\frac{\partial q}{\partial t} + u\,\frac{\partial C}{\partial z} = D_L\,\frac{\partial^2 C}{\partial z^2} \tag{1}$$

were C and q are the sample concentration in the mobile and stationary phases, respectively [10]. The volume ratio of stationary phase over liquid mobile phase is given by $F = V_a/V_0 = (1-\epsilon)/\epsilon$, where ϵ is the total porosity of the column. The parameter u is the average linear velocity and t and z are the time and position in the column, counting from the start of the injection, which is made at the column inlet.

This equation must be completed by a second one, relating the two functions of t and z in Eq. (1), the liquid and solid phase concentrations. The nature of this second equation is different in the two models used here.

2.1.2. Equations in dimensionless coordinates

In order to eliminate the spurious effects associated with changes in the values of geometrical parameters and to facilitate comparisons, it is convenient to use dimensionless values to characterize the importance of the two contributions to band broadening. Therefore, the apparent Peclet number, Pe, is used to describe the band broadening due to axial dispersion and the apparent Stanton number, St, is used to describe the dispersion due to mass transfer kinetics. The definitions of these new parameters are as follows:

$$\mathrm{Pe} = \frac{uL}{D_L}, \quad \mathrm{St} = \frac{k_f L}{u} \tag{2}$$

The dimensionless distance and time are $x = z/L$ and $\tau = ut/L$, respectively. With these definitions, Eq. (1) becomes:

$$\frac{\partial C}{\partial \tau} + F\,\frac{\partial q}{\partial \tau} + \frac{\partial C}{\partial x} = \frac{1}{\mathrm{Pe}}\,\frac{\partial^2 C}{\partial x^2} \tag{3}$$

Below, both contributions to band broadening are discussed independently of each other.

2.1.3. Band broadening in the transport model

There are two types of contributions to band broadening which are usually considered in liquid

chromatography, axial dispersion and the mass transfer resistances [10]. The former results from axial and eddy diffusions. It is included in the mass balance equation (Eq. (1)), being accounted for by the axial dispersion coefficient D_L. The contribution of a finite rate of the mass transfer kinetics is accounted for by the following kinetic equation, called the solid film linear driving force model, which assumes that the driving force for the mass transfer is proportional to the difference q^*-q in which q^* is the solid phase concentration in equilibrium with the liquid phase concentration C (see below, isotherm equation)

$$\frac{\partial q}{\partial t} = k_f(q^* - q), \quad \frac{\partial q}{\partial \tau} = \mathrm{St}(q^* - q) \tag{4}$$

where k_f is the mass transfer coefficient and St the corresponding value of the Stanton number. The combination of Eq. (3) and Eq. (4) constitutes the transport–equilibrium model [10]. In the simpler transport model, the one that was used in this work, it is assumed that $D_L = 0$ and the contribution of axial dispersion is lumped with that of the mass transfer kinetics. This is justified in the present case because the contribution of axial dispersion, which originates in the mobile phase, is quite small compared to that of the mass transfer resistances [6,7].

The experimental data (i.e., the breakthrough curves) are fitted to this model by looking for the value of St which gives the calculated breakthrough curve closest to the experimental one. As this is a univariate fitting problem, the determination of the best St is simple and rapidly done.

2.1.4. Band broadening in the equilibrium–dispersive model

In this model, all contributions to band broadening are lumped together into one single contribution, accounted for by an apparent axial dispersion coefficient, D_a. This coefficient replaces D_L in Eq. (1). The sample compound is assumed to be always in equilibrium between the stationary and mobile phase, therefore $q^* = q$ or $k_f \to \infty$ and Eq. (2) vanishes. The apparent axial dispersion coefficient is used as a convenient measure of the band broadening. It is related to the column efficiency through:

$$D_a = \frac{\sigma^2}{2t_0} = \frac{HL}{2t_0} = \frac{uL}{2N} \tag{5}$$

where σ^2 is the band variance, t_0 the hold-up time, H the column HETP, L the column length, N, the plate number, and $2N = \mathrm{Pe}$, where Pe is the column Peclet number ($\mathrm{Pe} = uL/D_a$) Eq. (2), not to be confused with the reduced velocity, equal to the particle Peclet number, ud_p/D_m, with D_m molecular diffusivity of the solute in the mobile phase), which can also be used to measure the extent of band broadening.

As explained in the previous subsection, the best values of Pe or D are conveniently derived by fitting the experimental breakthrough curve to the model, using parameter identification.

2.2. The adsorption isotherm

Because this model fitted properly the experimental data (see later), the Langmuir model was used in all theoretical calculations to represent the adsorption equilibrium:

$$q^* = \frac{aC}{1 + bC} \tag{6}$$

where q^* is the concentration of the compound in the stationary phase at equilibrium with a solution of concentration C in the mobile phase. a and b are numerical coefficients. The quotient a/b represents the saturation capacity, q_s, of the stationary phase or monolayer capacity. The coefficient b is related to the binding energy.

2.3. The plate height

The plate height, H, or HETP, is often used to describe band broadening in linear chromatography. With proper care, this concept can be extended to the case of nonlinear chromatography [10]. Thus, in order to calculate the plate height from the experimental breakthrough curves, the following equations were used. With the equilibrium–dispersive model and using the best value of Pe derived as explained earlier, we have

$$H_{\mathrm{Pe}} = \frac{2L}{\mathrm{Pe}} \tag{7}$$

With the transport model and using the best value of

St derived as explained earlier:

$$H_{St} = \frac{K}{(1+K)^2}\frac{2L}{St} \quad (8)$$

The original forms of these equations were derived for linear chromatography. It has been shown, however, that they can be extended to the nonlinear case by using the retention factor under nonlinear conditions [10], given by

$$K = F\frac{\partial q}{\partial C} = \frac{Fa}{(1+bC)^2} \quad (9)$$

The second of these two equations (Eq. (9)) corresponds to the particular case of a Langmuir isotherm (Eq. (6)). Note that in the linear case ($b=0$) this equation reduces to $K=Fa$. In this case the parameter K is identical to the classical retention factor $k'=(t_R-t_0)/t_0$ and we obtain the equation valid in linear chromatography.

Note that the values H_{St} and H_{Pe} are both lumped values. H_{Pe} includes the contribution of the mass transfer resistances (as they contribute to the apparent axial dispersion coefficient [10]) while H_{St} includes the (small) contribution of axial dispersion, for the same reason, that the transport model includes only one parameter for band broadening. The following modified Van Deemter equation was used in order to separate the dispersion from the kinetic contribution

$$H = A + C_s u \quad (10)$$

where

$$C_s = \frac{2K}{(1+K)^2 k_f} \quad (11)$$

with K given by Eq. (9), in the nonlinear case [10]. The modified Van Deemter equation used in this work (Eq. (10)) does not include the conventional B term which accounts for axial molecular diffusion. This term was eliminated because it is very small under the experimental conditions of this work. This decision is justified by the column efficiency reported earlier [6,7], which was 5000 theoretical plates for water and approximately 100 plates for Tröger's base.

2.4. Frontal analysis

Frontal analysis was used in this work for the determination of the adsorption isotherms and of either the apparent dispersion coefficient or the apparent rate coefficient of mass transfer. This classical method involves making step changes of increasing concentration at the column inlet and recording the resulting breakthrough curves. FA is the only chromatographic method that allows convenient and very accurate isotherm measurements when the column efficiency is low [11,12]. This is largely due to the formation of a self-sharpening front under the influence of a nonlinear thermodynamics of phase equilibrium. This effect causes the steepness of the front of the breakthrough curves to increase with increasing concentration. Solving the integral mass balance equation at each breakthrough curve gives one point of the isotherm [10,11]. Some other advantages of this method is that the injection volume is no longer a factor in determining the mass transfer coefficients and that it enables the investigation of a possible dependence of the front steepness on the concentration beside the self-sharpening effect due to a nonlinear isotherm.

2.5. Initial and boundary conditions

The initial and boundary conditions used in this work represent a staircase frontal analysis experiment. These Danckwerts conditions are written as follows [7,10,11]:

$$C(z,0) = C_{n-1}$$

$$uC(0,t) - D_L\frac{\partial C}{\partial z} = u(C_n - C_{n-1})$$

$$\frac{\partial C}{\partial z}(L,t) = 0 \quad \text{for } t \geq 0 \quad (12)$$

Initially, the column is filled only with pure mobile phase and contains no sample (i.e., $C_{n-1}=0$). Then a series of successive steps of increasing concentrations are injected into the column.

3. Experimental

3.1. Equipment

An HP 1090 liquid chromatograph (Hewlett-Pac-

kard, Palo Alto, CA, USA) equipped with a temperature-controlled column oven, a multi-solvent delivery system, an automatic sample injector, a diode array detector and a computer data acquisition system was used in this study. It has been previously shown that this equipment gives accurate composition of a stream of mobile phase obtained by mixing two solutions in set proportions and accurate step gradients [12]. These characteristics are of critical importance for performing reliable frontal analysis experiments.

3.2. Materials

3.2.1. Stationary phase

The microcrystalline CTA was obtained from Merck (Darmstadt, Germany). The 15–35 μm particle material was packed in a stainless-steel column (25×0.46 cm), using a slurry technique.

1,3,5-Tri-*tert*.-butylbenzene (TTBB) was used to measure the column porosity as used in previous reports [6,7]. TTBB can be considered to be a non-retained compound on CTA. The number of theoretical plates obtained for the column for TTBB was 550. The total void volume measured for the column was 2.517 ml. The total porosity was calculated as 0.606 and the phase ratio as 0.650.

3.2.2. Mobile phase and chemicals

S-Tröger's base was purchased from Aldrich (Milwaukee, WI, USA), 1,3,5-tri-*tert*.-butylbenzene from Fluka (Buchs, Switzerland) and ethanol (200 proof) from Aaper Alcohol and Chemical Co. (Shelbyville, KY, USA). These chemicals were used as received.

3.3. Procedures

Prior to packing, the CTA was boiled in ethanol for 45 min to allow it to swell. The solution was then cooled to room temperature and decanted. The resulting suspension was treated in an ultrasonic bath for 5 min at ambient temperature and poured into the packing chamber. The column was packed under a maximum pressure of 275 bars, using 180 ml of ethanol as the pushing solvent.

All chromatograms were obtained using frontal analysis at 40°C, under isocratic conditions. Pure ethanol was used as the mobile phase. The experiments were carried out using the automatic solvent delivery system to generate different concentration steps. Ten equidistant concentration steps were performed for each flow-rate. The flow-rates used were 0.2, 0.4, 0.6, 0.8, 1.0, and 1.2 ml/min. The lowest concentration of Tröger's base used was 0.3 g/l. The detector was set at 305 nm. The sample was recycled by fraction collection and concentration and reused after each run.

4. Results and discussion

4.1. Adsorption isotherms

The adsorption isotherms were derived from the experimental breakthrough curves using the area method and the less accurate half-height method [11]. These experimental isotherms are shown in Fig. 1a (area method) and Fig. 1b (half-height method). The Langmuir equation provided an excellent fit for the experimental adsorption isotherm data, a result which is not surprising given the range of concentration within which measurements could be done ($bC<0.4$). The two Langmuir coefficients were obtained by nonlinear regression. Table 1 lists the best values of the numerical coefficients, a and b, and the standard deviations afforded by each method. The area method yields a more precise estimate of the adsorption isotherm. This can be seen easily by comparing the standard deviations of the two numerical coefficients obtained with both methods (Table 1). These deviations can also be seen in Fig. 1a,b, in which the differences in accuracy and precision of the two methods are well illustrated.

The difference between the best estimates of the isotherm coefficients yielded by the two methods is explained by the concentration dependence of the rate coefficient of mass transfer and by the unusually low efficiency of the CTA column. For both reasons, the half-height method is affected by systematic errors, as described by Sajonz et al. [11]. Systematic differences between the results given by the two methods were also noted at high flow-rates. The results obtained with the area method exhibited markedly lesser deviations at high flow-rates than

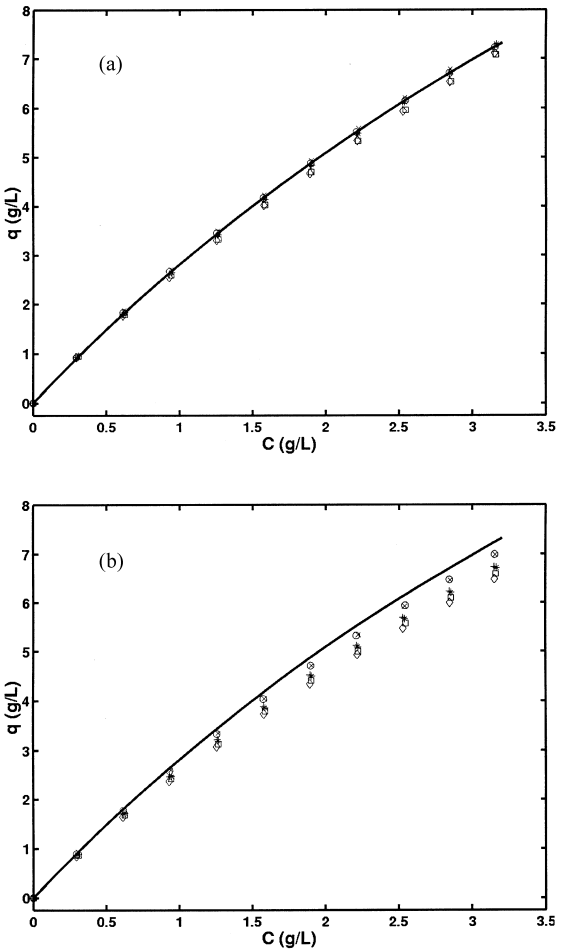

Fig. 1. Equilibrium isotherm of *S*-Tröger's base on cellulose triacetate. Experimental data (symbols) and best Langmuir isotherm (line). Flow-rates: 0.2 (○), 0.4 (×), 0.6 (+), 0.8 (*), 1.0 (□) and 1.2 (○) ml/min. (a) Data derived using the area method. (b) Data derived using the half-height method.

those obtained with the half-height method, in agreement with the earlier theoretical discussion [11].

4.2. Band broadening

The breakthrough curves obtained for each concentration step and flow-rate were fitted to breakthrough curves calculated as numerical solutions of Eq. (1) at different values of either the column Peclet number or the Stanton number, respectively (Eq. (3)). It was observed that it was always possible to obtain an excellent fit of a calculated breakthrough curve to an experimental curve, as illustrated in Fig. 2a–c which show the fittings for a flow-rate of 0.2 ml/min and for the initial, middle and final concentration ranges studied, respectively. As a consequence, an accurate estimate of the numerical value of corresponding apparent dispersion coefficient, D_a, could be obtained in all cases.

Table 1
Best coefficients of the Langmuir isotherm

Method	*a*	R.S.D. (*a*)	*b*	R.S.D. (*b*)
Area	3.139	0.016	0.116	0.002
Half-height	2.988	0.043	0.120	0.007

The same experimental data could also be fitted to the transport model which gave best values of the Stanton number. The quality of the fit obtained is illustrated in Fig. 3a–c which correspond to the same experimental data as those fitted to the equilibrium–dispersive model in Fig. 2a–c, respectively. The quality of the fits was the same for all the other experimental cases, irrespective of the concentrations and flow-rates used (not shown). Small differences always subsist between calculated and experimental breakthrough curves, especially in the high concentration range. These differences suggest that the mass transfer kinetics may be somewhat more complex than assumed in the equilibrium–dispersive model or even in the transport model. This is not surprising since both models are simplified and lump all contributions to band broadening into one single coefficient while it should be expected that the concentration dependences of these different contributions are not the same.

The values for all apparent Pe and St numbers and the corresponding HETP values, H_{Pe} and H_{St}, are listed in Table 2. Fig. 4a,b shows plots of these two HETPs versus the linear flow velocity of the mobile phase. Fig. 4a corresponds to the equilibrium–dispersive model and Fig. 4b to the transport model. In both cases, the HETP increases linearly with increasing flow velocity, as predicted by Eq. (8). It also decreases with increasing average concentration of the breakthrough step.

In order to separate the band broadening contributions due to slow mass transfer and to axial dispersion, the calculated values of the HETP were fitted to a modified Van Deemter equation (Eq. (8)). The fact that the dependence is linear shows that the range of values of the reduced flow velocities under which the

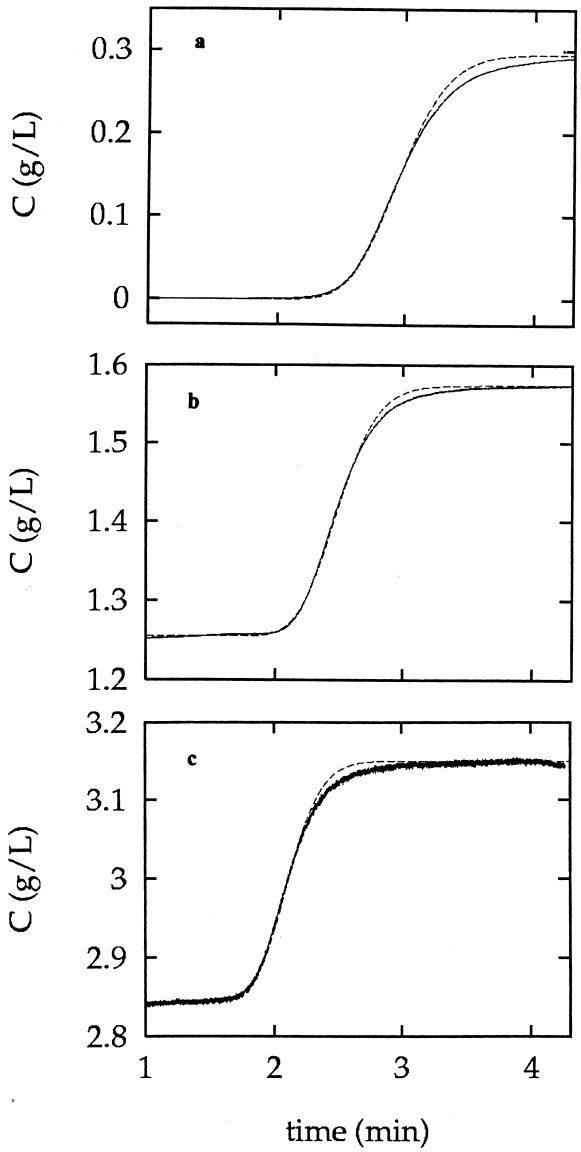

Fig. 2. Illustration of the procedure used for the determination of the Peclet number. Comparison between the experimental breakthrough curves (solid line) and calculated curves (dotted and dashed lines). Flow-rate, 0.2 ml/min. (a) $C_n=0.00$, $C_{n+1}=0.29$, Pe=150. (b) $C_n=1.25$, $C_{n+1}=1.57$, Pe=170. (c) $C_n=2.84$, $C_{n+1}=3.15$, Pe=180.

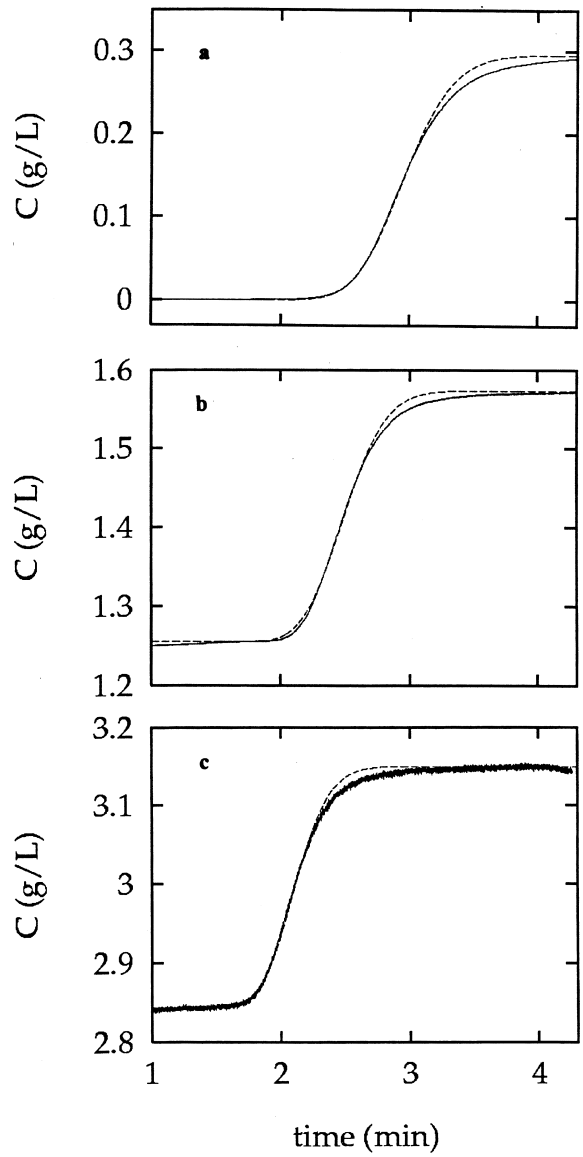

Fig. 3. Illustration of the procedure used for the determination of the Stanton number. Comparison between the experimental breakthrough curves (solid line) and calculated curves (dotted and dashed lines). Flow-rate, 0.2 ml/min. (a) $C_n=0.00$, $C_{n+1}=0.29$, Pe=35. (b) $C_n=1.25$, $C_{n+1}=1.57$, Pe=40. (c) $C_n=2.84$, $C_{n+1}=3.15$, Pe=45.

experiments were carried out was large enough to allow neglecting the B term (molecular diffusion) in this equation, as indicated earlier. In other words, the minimum of the Van Deemter curve takes place at a flow-rate markedly lower than 0.2 ml/min. The mass transfer rate coefficients and the axial dispersion coefficients were derived from the slope and intercepts of the straight lines in Fig. 4a and Fig. 4b, respectively. The results are listed in Table 3. The values of k_f obtained by the two methods are in excellent agreement, illustrating the consistency of the two approaches. These values increase by ap-

Table 2
Best values of the apparent Peclet and Stanton numbers

Flow-rates (ml/min)	C_n (g/l)	C_{n+1} (g/l)	Pe	H_{Pe} (cm)	St	H_{St} (cm)
0.2	0.00	0.29	150	0.333	35	0.319
	1.25	1.57	170	0.294	40	0.299
	2.84	3.15	180	0.277	45	0.277
0.4	0.00	0.31	120	0.416	25	0.446
	1.26	1.58	130	0.384	30	0.400
	2.85	3.15	140	0.357	32	0.389
0.6	0.00	0.30	90	0.556	20	0.558
	1.26	1.57	100	0.500	24	0.500
	2.84	3.14	110	0.454	26	0.479
0.8	0.00	0.31	70	0.714	18	0.660
	1.26	1.58	80	0.625	20	0.610
	2.85	3.16	90	0.556	24	0.523
1.0	0.00	0.31	60	0.833	14	0.798
	1.26	1.58	70	0.714	16	0.750
	2.85	3.15	80	0.625	20	0.622
1.2	0.00	0.29	50	1.00	12	0.930
	1.25	1.57	60	0.833	14	0.856
	2.84	3.14	70	0.714	15	0.779

proximately 60% in the concentration range investigated. This concentration range was yet rather moderate since the largest value achieved for the product bC, which is a measure of the deviation of the isotherm from linear behavior, was only 0.40. This result confirms the strong apparent dependence of the mass transfer rate coefficient on the concentration previously reported [11–13].

5. Conclusion

Our results confirm that the area method is more precise and more accurate than the conventional half-height method for the calculation of the retention times of breakthrough curves and the determination of isotherm data by frontal analysis. The latter method should never be used when the column efficiency is significantly lower than 1000 theoretical plates.

Both the equilibrium–dispersive model and the transport model of chromatography can be used for the study of band-broadening effects in frontal chromatography. Both models give essentially the same results. By applying the classical Van Deemter model the mass transfer and axial dispersion coefficients can be obtained independently. In principle, the same result could have been obtained by using directly the transport–diffusive model (Section 2.1.2). However, the simultaneous determination by parameter identification of the two coefficients, D_L (Eq. (1)) and k_f, instead of only one could not have been sufficiently accurate.

Finally, the experimental results reported in this

Table 3
Estimates of the Van Deemter coefficients

	C_n (g/l)	C_{n+1} (g/l)	A (cm)	C_s (1/min)	k_f (1/min)	Pe
H_{St}	0.0	0.3	0.1945	0.0600	7.44	268.8
	1.3	1.6	0.1740	0.0566	8.47	287.4
	2.8	3.2	0.1860	0.0467	10.60	257.1
H_{Pe}	0.0	0.3	0.1617	0.0437	6.66	309.2
	1.3	1.6	0.1727	0.0538	8.91	289.5
	2.8	3.2	0.1843	0.0670	11.40	271.3

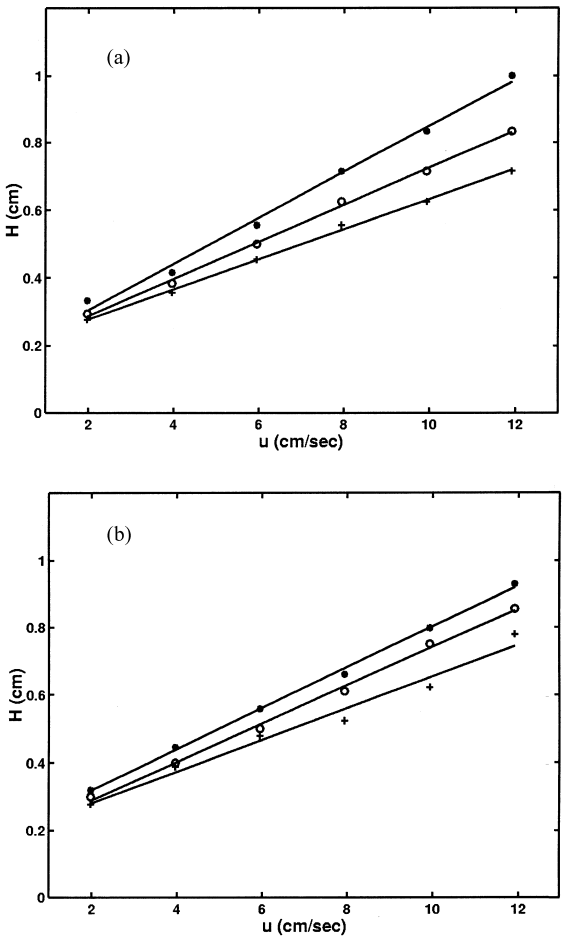

Fig. 4. Dependence of the plate height on the flow velocity. The data for three concentration steps only have been considered. Concentration steps: 0.0–0.30 g/l (*), 1.25–1.55 g/l (o), and 2.84–3.15 g/l (+). (a) Equilibrium–dispersive model. (b) Transport model.

work confirm the important concentration dependence of the mass transfer of the *S*-Tröger's base in CTA [8], a dependence that seems now to be a general result [8,9,13].

Acknowledgements

This work has been supported in part by grant CHE-9701680 of the National Science Foundation and by the cooperative agreement between the University of Tennessee and the Oak Ridge National Laboratory. We thank Torgny Fornstedt (BMC, University of Upsala, Sweden) and Andreas Seidel-Morgenstern (Otto-von-Guericke Universität, Magdeburg, Germany) for fruitful discussions. We acknowledge the support of our computational effort by the University of Tennessee Computing Center.

References

[1] G. Blaschke, J. Liq. Chromatogr. 9 (1986) 341.
[2] T. Shibata, I. Okamoto, K. Ishii, J. Liq. Chromatogr. 9 (1986) 313.
[3] A. Rizzi, J. Chromatogr. 478 (1989) 87–99.
[4] E. Francotte, A. Junker-Bucheit, J. Chromatogr. 576 (1992) 1.
[5] G. Hesse, R. Hagel, Chromatographia 6 (1973) 277.
[6] G. Guiochon, A. Seidel-Morgenstern, J. Chromatogr. 631 (1993) 37.
[7] A. Seidel-Morgenstern, G. Guiochon, Chem. Eng. Sci. 48 (1993) 2787.
[8] A. Seidel-Morgenstern, S.C. Jacobson, G. Guiochon, J. Chromatogr. 637 (1993) 19.
[9] H. Guan-Sajonz, P. Sajonz, G. Zhong, G. Guiochon, Biotechnol. Progr. 12 (1996) 380.
[10] G. Guiochon, S. Golshan-Shirazi, A.M. Katti, Fundamentals of Preparative and Nonlinear Chromatography, Academic Press, Boston, MA, 1994.
[11] P. Sajonz, G. Zhong, G. Guiochon, J. Chromatogr. A 731 (1996) 1–25.
[12] H. Guan, B.J. Stanley, G. Guiochon, J. Chromatogr. A 659 (1994) 27.
[13] P. Sajonz, H. Guan-Sajonz, G. Zhong, G. Guiochon, Biotechnol. Progr. 13 (1997) 170.